Available online at www.sciencedirect.com
SCIENCE DIRECT®
Journal of Nuclear Materials 352 (2006) 57–61
journal of nuclear materials
www.elsevier.com/locate/jnucmat

Oxide dispersion strengthened steel irradiation with helium ions

M.A. Pouchon *, J. Chen, M. Döbeli, W. Hoffelner

Laboratory for Materials Behaviour, Paul Scherrer Institute, OHLA/131, 5232 Villigen PSI, Switzerland

Abstract

Oxide dispersion strengthened (ODS) ferritic steels are investigated as possible structural material for the future generation of high temperature gas cooled nuclear reactors. ODS-steels are considered to replace other high temperature materials for tubing or structural parts. The oxide particles serve for interfacial pinning of moving dislocations. Therefore, the creep resistance is improved. In case of the usage of these materials in reactors, the behavior under irradiation must be further clarified. In this paper the effects induced by $^4He^{2+}$ implantation into a ferritic ODS steel are investigated. The fluence ranges from 10^{16} to 10^{17} cm^{-2} and the energy from 1 to 2 MeV. The induced swelling is investigated for implantations at room temperature and 470 K. It is derived from the irradiation induced surface displacement, which is measured with an atomic force microscope (AFM). With a displacement damage of 0.6 dpa, a volume increase of 0.65% is observed at room temperature and 0.33% at 470 K. A cross-sectional cut is performed by focused ion beam and investigated by transmission electron microcopy (TEM). The defect density observed on the TEM micrographs agrees well with the computational simulation (TRIM) of the damage profile.

PACS: 61.80.Lj; 61.80.−x; 07.10.Pz

1. Introduction

Because of the excellent thermal creep behavior, oxide dispersion strengthened (ODS) steels are considered as potential candidates for high temperature applications in fusion reactors [1,2] and high temperature fission reactors [3]. The ferritic alloy PM2000 is studied in this work, with its high chromium and aluminum content, this product is very similar to the MA956, except for being nickel free. The high aluminum content can be disadvantageous under certain conditions, especially for fusion applications. However, it plays an important role for corrosion protection in a high temperature gas cooled reactor, where some impurities in the cooling gas could lead to severe oxidation. In order to understand the swelling behavior of PM2000, an accelerator is used to implant $^4He^{2+}$ ions for producing a well defined damage profile into the specimen. The samples are then evaluated by a surface analysis. A verification of the assumed implantation profile, which is usually estimated from TRIM calculations (a computer code simulating the *tr*ansport of *i*ons in *m*atter, see [4]), is performed by a TEM investigation of an irradiated sample section.

* Corresponding author. Tel.: +41 56 310 2245; fax: +41 56 310 4595.
E-mail address: manuel.pouchon@psi.ch (M.A. Pouchon).

0022-3115/$ - see front matter © 2006 Elsevier B.V. All rights reserved.
doi:10.1016/j.jnucmat.2006.02.070

2. Experimental

2.1. PM2000 and sample preparation

For the present studies, the commercial product PM2000 from Plansee is used. Its composition is as follows: (wt%) 73.5 Fe, 20 Cr, 5.5 Al, 0.5 Ti, and 0.5 Y_2O_3, where the size of the dispersed Y_2O_3 particles ranges from 20 to 70 nm. It is manufactured by mechanical alloying in a high energy mill to produce a solid solution which contains a uniform dispersion of yttria. The powder is consolidated using hot isostatic pressing followed by a hot and cold rolling procedure. A thermal treatment finalizes the production [5,6].

Samples measuring $6 \times 6 \times 1\ mm^3$ are cut in a long transverse direction. One face is ground with SiC papers down to a P-grading of 4000. A polishing with 6 and 3 μm diamond suspensions follows; the polishing is finalized with a SiO_2-suspension (OP-S).

2.2. He irradiation

Polished PM2000 plates are irradiated with He ions through a 400 mesh TEM-grid. Because of the partial shading from the grid, an alternating irradiated/non-irradiated pattern is generated on the sample. In order to obtain an even displacement dose distribution as a function of depth, two different methods are used. For the irradiation only being performed at room temperature, the incident angles are varied from 0° to 66° at a constant He ion energy of 1.5 MeV (see Fig. 1(a)) for more details

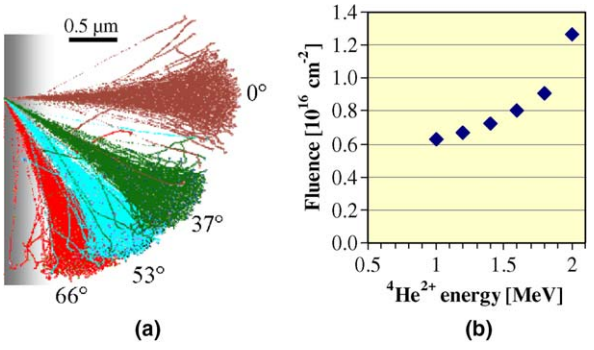

Fig. 1. Implantation conditions: (a) TRIM *XY* longitudinal projection of the irradiation performed under four different incidence angles. Only applicable at room temperature. (b) Fluences being used to achieve an even displacement dose distribution in depth for the implantation series, where the energy is varied. This irradiation technique was applied for one measurement at room temperature and one at 470 K.

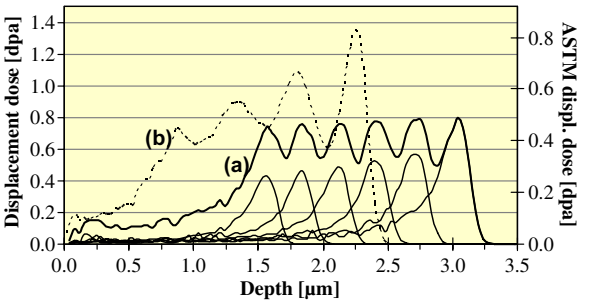

Fig. 2. Implantation profiles: (a) Damage profile for an irradiation with He ions of 6 different energies, ranging from 1.0 to 2.0 MeV, for the fluences see Fig. 1(b). Bold line: sum of all energies; thin lines: single energies. The total fluence is $5.0 \times 10^{16}\ cm^{-2}$. (b) Dotted line: damage profile of the implantation performed under four different incident angles, see Fig. 1(a) and [3]. The total fluence is $5.6 \times 10^{16}\ cm^{-2}$. The left *Y*-axis represents the dpa values calculated with the TRIM default displacement energies, and the right *Y*-axis according to ASTM recommendations [7].

on this technique, and also on the accelerator being used see [3]. The resulting irradiation profile is shown in Fig. 2(b).

When using a furnace during irradiation, the variation of the incidence angle is not possible in the presently used experimental arrangement. Therefore, a second irradiation series is performed, where the He ion energy is varied in 200 keV steps from 1.0 to 2.0 MeV. For comparison with the irradiations performed under varying incident angles, an irradiation is performed at room temperature. The second irradiation is performed at 470 K. The variation in fluence is shown in Fig. 1(b) and the resulting displacement dose profile in Fig. 2(a). It is obvious that the latter implantation results in a thicker layer at the surface, which is almost not damaged. Only at a depth of 1.25 μm the displacement dose starts to increase significantly. The dpa profiles in Fig. 2 have been calculated with the default displacement energies given in TRIM (25 eV for Fe, Cr, Al, Ti and Y, 28 eV for O). A second simulation was performed with values given by an ASTM norm [7]. In this reference the recommended displacement energies for Fe and Cr are 40 eV and for Ti 30 eV. The other values are not changed. The resulting damage is represented in the right *Y*-axis. The displacement energy depends very much on the crystal structure and orientation. In [7] for example, besides the recommended displacement energy of 40 eV for Fe, a threshold value of 20 eV is given for a polycrystalline specimen. In the present paper, the dpa values derived with the

default TRIM setup, are taken as reference, however, the dpa values can easily be transformed into the ones being derived with the displacement energy value given in [7] (multiplying with 0.61).

2.3. Surface evaluation

The surface elevation is investigated using an atomic force microscope (AFM). Because the pattern structure is one-dimensional, the two-dimensional surface information can be averaged in the perpendicular direction. The surface quality of the samples is disrupted by the oxide inclusions. These disruptions are visible as peaks in the AFM images. They are removed by an automated peak removal algorithm before averaging the elevation information. For a detailed description and an example of a resulting step profile see [3]. Several AFM evaluations are performed on each irradiated sample. In case of the multi-angle implantation, an iterative method is used, in order to calculate the effective strain from the surface displacement data. This is necessary, because the damage profile (see Fig. 2(b)) is not constant in the region being evaluated (from 0.5 to 2.5 μm). Together with the non-linearity of the strain response as function of displacement damages per atom (dpa), this implies the necessity of an iterative process, where the strain to dpa curve is adjusted according to the recalculated surface displacement, as referred earlier [3].

In case of the implantation with varying energies and an incident angle of 0°, a depth region of 1.25 to 3.25 μm is relevant for swelling (see the implantation profile 2(a)). The irradiation according to 2(a) resembles more a step function than 2(b). Therefore, the strain can be calculated from the proportion of the surface displacement to the thickness of the mainly damaged layer.

2.4. TEM evaluation of the irradiation profile

The irradiated area is investigated by TEM. For verification of the assumed irradiation profile, a lamella of nominally 100 nm thickness oriented perpendicular to the surface is extracted from the irradiated sample, using a focused ion beam (FIB). TEM the extracted lamella of 5×7 μm^2 is very constant in thickness and transparent to the electron beam on the entire lamella. Under these circumstances, the integral of the defects results in a reduction of the transmittance to the electron beam. The transmittance change as a function of the defect density is not exactly known, however it is assumed that there is a monotonous relation analogous to photographic films, which saturates at high defect densities. With this assumption the transmittance of the TEM pictures (negative of bright field exposure, see Fig. 5) is averaged in parallel direction to the surface. As a result, a depth dependent transmittance function is obtained and compared to the TRIM simulation. The grayscale values observed on the image, are relative values, and do not deliver an absolute measure of the displacement dose. The transmittance of the negative film is also influenced by the parameter settings in the electron microscope and later in the settings of the negative scanner. Furthermore, the signals on the TEM reflect the surviving defects, which are much less than the initially displaced atoms. The film thickness and many other factors also influence the contrast.

3. Results and discussion

3.1. Surface displacement/swelling

Fig. 3 shows the surface displacement measured on the sample irradiated with the profile shown in Fig. 2(a). At room temperature the surface elevation is (13.1 ± 1.8) nm, and at 470 K it is (6.6 ± 0.5) nm. This result is qualitatively in agreement with the theory, where the radiation induced interstitials and clusters, potentially causing a volume expansion, are recombining at an increasing temperature [8]. In the low temperature region (starting from 0 K) the surviving defects sharply decrease with increasing temperature, for the pure copper investigated in [8] at $T/T_M = 0.2$ this effect saturates, and the surviving defect density remains constant (T, temperature in K; T_M, melting temperature in K). At about the same relative temperature, the vacancies start to be mobile, which would explain the void

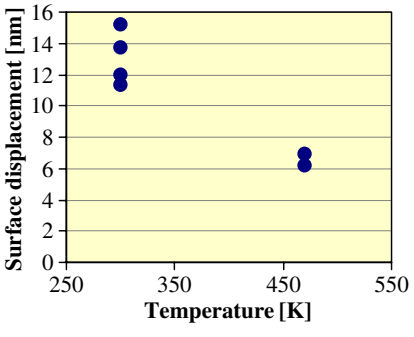

Fig. 3. Temperature dependent surface displacement data.

formation at higher temperatures. Therefore, the swelling observed in this paper is not the void swelling normally observed, but an interstitial/cluster induced volume increase, in the low temperature region. The typical temperatures where the interstitials and the vacancies are mobile, are only given for copper in [8], but are not known for the material being investigated here; therefore, this can only be a preliminary explanation, and the effect has to be further investigated.

The calculation of the strain data found with the multi-angle implantation can be found in [3]. In case of the multi-energy implantation, the strain can be calculated for the relevant 2 μm layer to be $(0.65 \pm 0.15)\%$ at room temperature and $(0.33 \pm 0.03)\%$ at 470 K.

Fig. 4 shows the data obtained from both implantation profiles. The data obtained with the other implantation profile is about 30% lower than the values found with the former implantation profile. The reason could be the larger surface layer, with a very small displacement dose. If the displacement dose is low enough, this layer could constrain the underlying swelling region. Beyond a threshold of displacement dose the irradiation creep is sufficient, that all swelling is released perpendicular to the surface [9].

Therefore, the swelling can directly be related to the surface displacement data divided by the irradiated layer thickness. In an unconstrained, non-creeping system, the swelling data is the triple value of the surface displacement (for a relatively small surface displacement, the relative volume increase is three times the relative surface displacement).

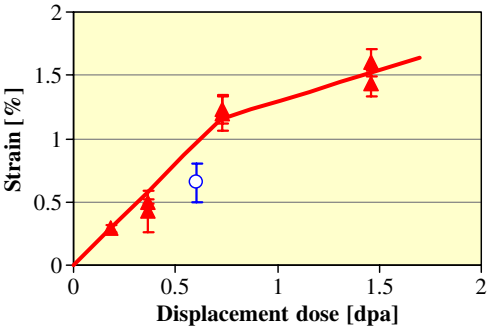

Fig. 4. Strain data at room temperature as a function of the average displacement dose in the relevant 2 μm layer.
○: Strain data derived from the irradiation profile described in Fig. 2(a). The depth range from 1.25 to 3.25 μm is taken as relevant layer for the surface displacement of 13.1 ± 1.8 nm (see Fig. 3).
▲: Strain data resulting from the irradiation profile depicted in Fig. 2(b), this data is calculated from the surface elevation with the correction method described in [3], and includes the trend-line.

3.2. Depth profile analysis

Fig. 5 shows the TEM image of a lamella extracted perpendicular to the surface. Under the micrograph, the averaged transmittance of the image is plotted as a function of depth. The TRIM data of the first irradiation series is overlaid on this density data. To reach an agreement, an 11% stretching in depth of the TRIM curve is necessary. Only black dots (interstitial and vacancy clusters) will contribute to the change in the optical density of the TEM image. Therefore, the TEM picture is compared to the displacement dose and not to the

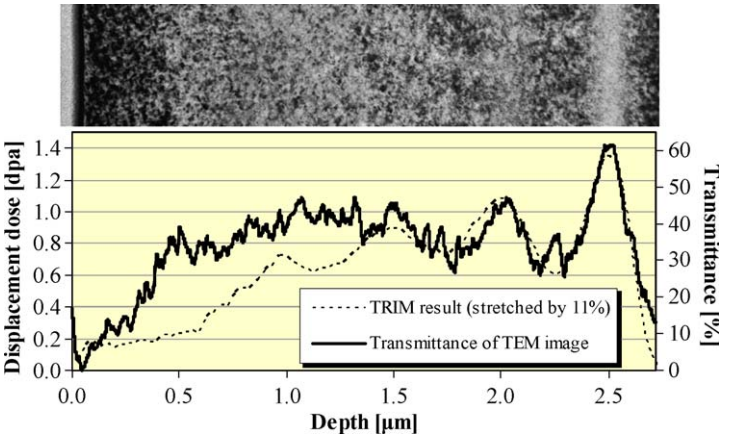

Fig. 5. TEM picture of the lamella extracted by FIB. The left side represents the specimen surface. In the lower part the averaged transmittance of the TEM is plotted as a function of depth. The TRIM simulation is overlaid. See the text for details.

He concentration. The two most intense displacement peaks in the TRIM simulation well comply with the transmittance of the TEM. The difference of 11% in depth can partially come from the inaccuracy of the semi-empirical model used by TRIM. A possible explanation for the difference in the shallow implantation region of the first micrometer is the very flat incident angle of 66°, see Fig. 1(a). In this case even a slight deflection effect would importantly change the characteristics of the profile in this regime.

4. Conclusions

For ODS irradiated with $^4He^{2+}$ the swelling reduction with increasing temperature, in the regime from room temperature to 470 K, can be explained with the increased number of interstitials/clusters recombination. The often stated void swelling becomes only important at higher temperatures, and is not addressed in this study. Two different implantations profiles were applied, once under varying incidence angles, and once with a range of different energies. In the former case an iterative calculation method has to be developed, to extract the strain data from the surface displacement. In the latter case, the profile resembled much a step function, and a straightforward calculation is performed. The strain derived from the two implantation profiles at room temperature differs roughly by 30%. The smaller surface displacement signal in case of the multi-energy implantation can be explained with the larger, only slightly damaged layer above the swelling region, this might constrain and blur the displacement at the surface. The comparison of the profile obtained by using TRIM with the TEM picture of the lamella, results in a good agreement of the two most distinct intensity peaks. However, a stretching of the TRIM profile by 11% is necessary. Additionally the near-surface region shows more defects than expected from TRIM. Both profiles are still very similar, and it is abstained from a correction of the strain data obtained for the multi-angle implantation. For this minor change, the differences have to be confirmed by more experiments. On the other hand these experiments confirm the potential of this type of small scale experiments, in which two different irradiation profiles lead to very similar results.

Acknowledgements

The authors gratefully acknowledge Mr Joy Tharian (EMPA, Dübendorf, Switzerland) for the extraction of the lamella from the irradiated ODS sample, using the focused ion beam, Mr Rolf Schelldorfer (Paul Scherrer Institute, Villigen, Switzerland) for performing the scans with the atomic force microscope and Mr Tomislav Revac (Paul Scherrer Institute, Villigen, Switzerland) for the sample preparation.

References

[1] M.B. Toloczko, F.A. Garner, C.R. Eiholzer, J. Nucl. Mater. 258–263 (1998) 1163.
[2] M.B. Toloczko, D.S. Gelles, F.A. Garner, R.J. Kurtz, K. Abe, J. Nucl. Mater. 329–333 (2004) 352.
[3] M.A. Pouchon, M. Döbeli, R. Schelldorfer, J. Chen, W. Hoffelner, C. Degueldre, in: Proceedings of 16th International Conference on Physics of Radiation Phenomena and Radiation Material Science (Alushta, Crimea, 3–7 September, 2004), (VANT, Voprosy Atomnoi Nauki i Techniki, ISSN 1562-6016), vol. 3 (86), 2005, p. 122.
[4] J.F. Ziegler, J.P. Biersack, U. Littmark, The Stopping and Range of Ions in Solids, Pergamon, New York, 1985.
[5] Dispersion-strengthened High-temperature Materials/Material Properties and Applications, Prospectus from Plansee, 2003, 706 DE.04.03(1000)RWF.
[6] A. Czyrska-Filemonowicz, B. Dubiel, J. Mater. Process. Technol. 64 (1997) 53.
[7] ASTM Designation: E 521 – 96, Neutron Radiation Damage Simulation by Charged-Particle Irradiation, 1996.
[8] W. Schilling, H. Ullmaier, Physics of Radiation Damage in SolidsMaterials Science and Technology, Nuclear Materials, vol. 10B, Wiley, 1996, p. 225.
[9] F.A. Garner, D.S. Gelles, J. Nucl. Mater. 159 (1988) 286.